The 2017 World Congress on
Advances in Structural Engineering and Mechanics (ASEM17)
28 August - 1 September, 2017, Ilsan(Seoul), Korea

Health condition simulation of rail weld in high-speed railway based on geometric gradient and axle-box acceleration

Ping Wang [1)] , Bo-Yang An [2)] , Jie-Ling Xiao [3)] , *Jing-Mang Xu [4)] and Rong Chen [5)]

[1), 2), 3), 4), 5)] *Key Laboratory of High-speed Railway Engineering, Ministry of Education, Southwest Jiaotong University, Chengdu 610031, China*
[4)] *mang080887@163.com*

ABSTRACT

Due to the limitation of welding process and material heterogeneity, short wave length irregularity can easily occur in rail weld and inspire high wheel-rail force, whose geometric size should be strictly controlled. Compared with the traditional measure to control wave length or depth, method assessing rail weld by geometric gradient can consider local irregularity. However, this method should be calibrated by numerical simulation to establish a quantitative relationship between geometric gradient and wheel-rail force. This paper employed a 3D transient wheel-rail rolling contact model based on explicit finite element method to create such relationship, through simulating wheel-rail dynamic interaction at theoretical rail welds under 200~400 km/h. The study found intervention values acquired from numerical simulations were quite close to that in used, which validated the accuracy and reliability of the numerical model, and further proposed critical value of 400 km/h. A quantitative relation between axle-box acceleration and wheel-rail force had also been established, which can be directly used in engineering application to assess dynamic force at rail weld. Based on measured rail weld geometries, it investigated wheel-rail interaction at these irregularities and discussed their force transition in the whole life. Results of this paper can lay a theoretical basis and data support for the maintenance of railway departments.

1. INTRODUCTION

Rails of standard length can be welded into rails of required length in the continuous welded track to eliminate the joint gaps. This method is able to improve the continuity and integrity of the track structure, provide a good riding performance, extend service life of rails and decrease labor in maintenance, which has been widely developed in the railway. However, the geometrical dimensions at the rail welds are difficult to maintain due to the limitation of the welding process and the improper

---

[1)] Professor, [2)] Ph. D, [3)] Lecturer, [4)]Postdoc, [5)] Associate Professor

operation, the phase transformation between welding materials and base metals, as well as the influence of residual stress and fatigue crack. (Gao 2016) conducted a detailed investigation on the geometric irregularity of rail welds in China's high-speed lines and found that the shortwave irregularity is a main form of surface defects in the rail weld zones.

When the wheel is rolling on the rail in a steady state, the system deformation is in equilibrium with the applied constant load. The balance will be broken due to the existence of rail weld irregularities, and stimulates a higher wheel-rail force, resulting in the collapse of the rail weld, rail corrugation and even broken rail. Therefore, controlling the size of weld irregularity is of great importance to ensure secure, stable and economic operation of high-speed railway. In China, the straightness shall not exceed 0.3mm and 0.2mm at the operating speeds of 200km/h and 300km/h, respectively, within the straightedge measuring range of 1m in Chinese maintenance regulation for high-speed ballastless track lines. Obviously, this standard ignores the influence of geometrical wavelengths on wheel-rail force. (Xiao 2010) 's researches show that the wheel-rail force at the rail weld increases with the decrease of the wavelength, and propose safety limits under different speed against the irregularity of rail welds based on dynamics index or dynamic factors. However, weld irregularities were modelled as ideal cosine waveform in these studies, which are usually different from the actual weld geometry. Thus, conclusions of the above researches are difficult to be applied in the maintenance of actual lines. Unlike the depth limits proposed for a certain wavelength with utilization of ideal geometries, (Steenbergen 2006) evaluated the quality of the rail welds using a geometric gradient which can be used for considering any weld geometric forms. Also, related standards have been determined on the basis of numerical calculation and engineering experience. But this standard only established based on the linear relation between geometric gradient and dynamic force to satisfy engineering requirements with the dynamic force 11 kN as a limiting indicator of track quality evaluation for new built lines or after grinding maintenance. 90kN is generally regarded as the safety limit to control the dynamic interaction of wheels and rails in daily operation. Therefore, it shall establish a more precise relationship between geometric gradient and dynamic force to serve the maintenance of the railway department.

The premise of carrying out the evaluation of wheel-rail force at rail welds stated in the last paragraph is to obtain its geometric size, which generally is high time and manpower consuming. By contrast, detection of axle box acceleration is a simple and economical method, whose advantage is that accelerometer can be easily installed on existing standard vehicles without limitation of running speed of vehicles (Grassie 1996). Thereby, international scholars have made attempts to reflect the health status of track system through the response of axle box acceleration. (Liang 2013) has developed a set of indoor rolling test device for simulating the response of axle box acceleration at speed conditions ranging from 3.5 to 15 km/h when there are flaws on the wheel-rail surface. Obvious fluctuations of axle box acceleration were generated at the damages. (Molodova 2016) carried out corresponding tests of axle box acceleration (with the vehicle speed of 100km/ h) against some damages occurring at weld joints on site with preliminary establishment of a health monitoring system that can detect components in bad service statuses. (Molodova 2011) simulated the changes of axle

acceleration at short-wave irregularities of rail at a speed of 140 km/h by using 3D explicit finite element model and results conforming to the site test were obtained. It shall be noted that main purpose of above studies was to monitor defects through the dynamic response in time and frequency domain. Thus, the relationship between the axle box acceleration and the wheel-rail force was not given, and axle box acceleration cannot be quantitatively used to limit dynamic force at rail weld.

In the past, the calculation of wheel-rail force was widely used in the multi-body dynamic model (Steenbergen 2006, Xiao 2010). However, the wheelset was generally considered as a rigid body in this method, so that the axle box acceleration cannot be obtained. To overcome this problem, a 3D wheel-rail rolling contact model is developed in this paper based on the explicit finite element method, and applied to solve the dynamic interaction at the theoretical and measured rail welds. A detailed outline of this paper is presented in section 2.1.

2 METHOD FOR EVALUATING HEALTH CONDITION AT RAIL WELD

2.1 Overview of the method and outline of this paper

A method for evaluating health condition of rail weld is shown in Fig. 1. By introducing a series of theoretical geometries described in section 2.2, dynamic response of wheel-rail interaction at rail welds are solved through employing a 3D rolling contact finite element model, and three relations are thus proposed. The first, based on QI method (Steenbergen 2006) briefly introduced in section 2.3 and numerical results in section 3.1, intervention values considering speed range 200~400 km/h are obtained for application to quality assessment at new rail weld. The second, it creates a dynamic force map for wheel-rail force evaluation and evolution at rail weld under 300km/h, and it is explained in detail considering several measured rail weld irregularities in section 3.2 and 3.3. The last, a quantitative relation between axle box acceleration and wheel-rail force is acquired for evaluating health condition at rail weld through measured axle box acceleration, see section 4. Hence, we can detect health condition of rail weld based on measured geometric gradient and axle-box acceleration.

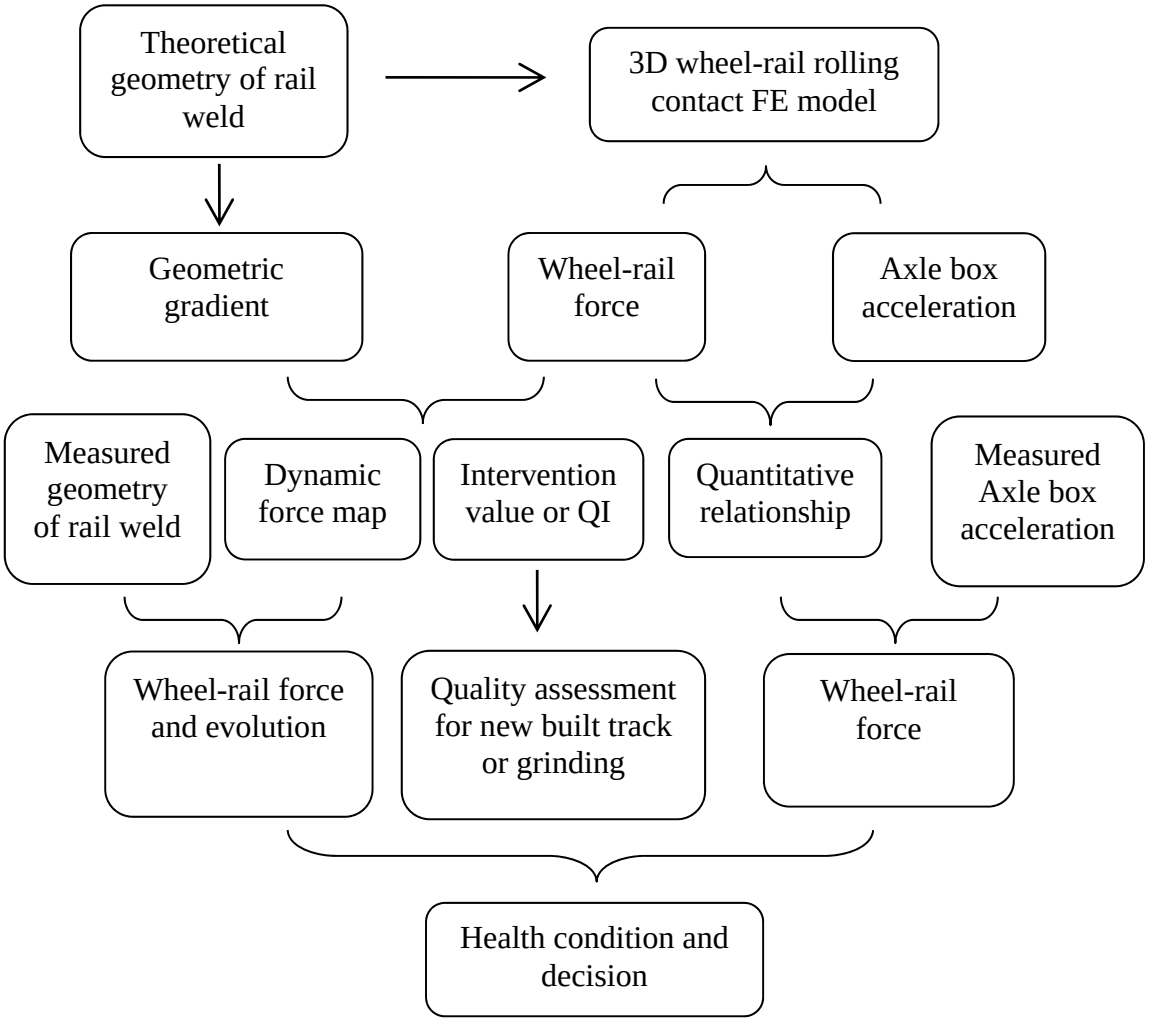

Fig. 1 Schematic diagram of the method

2.2 Theoretical geometry and its gradient

For easy understanding, the theoretical geometry is adopted to simulate the rail weld irregularity in this section,

$$z = \frac{\delta}{2}(1+\cos\frac{2\pi x}{\lambda}) \tag{1}$$

Where, δ and λ are the wave depth and length of the weld; *x* and *z* follow the longitudinal and vertical direction.

First-order derivative is solved from (1) to obtain the geometric gradient's expression of theoretical weld,

$$\frac{dz}{dx} = -\frac{\delta\pi}{\lambda}\sin\frac{2\pi x}{\lambda} \tag{2}$$

Taking 1m wavelength as an example, the cosine-shaped weld geometry and its gradient change are presented in Fig. 2 with the wave depth obtained as 0.2 mm. As *z* increases, the gradient shows a sine change, reaching the maximum at the 1/4 wavelength of the weld. When the gradient is greater than zero, *z* increases with the

increment of the longitudinal coordinate; and when the gradient is negative, the change is on the contrary. Thus, the three zero-point points of the gradient are corresponded to the starting point, peak and end point of rail weld, respectively. The first two of these points obviously determine the depth *d*, which triggers an approach defining the characteristic depth of measured rail weld and it is presented in section 3.2 for engineering application.

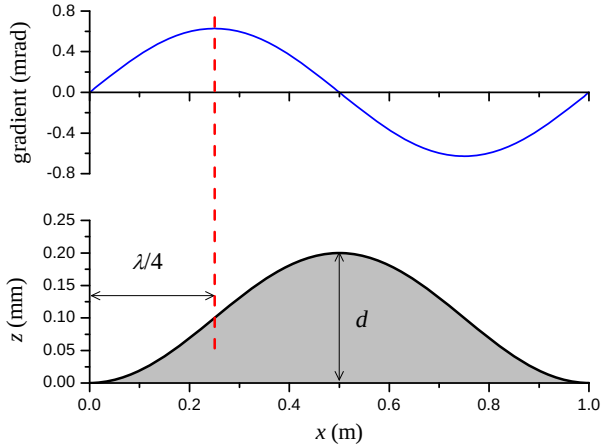

Fig.2 Rail weld geometry and its gradient change

As mentioned in the introduction, the maximum straightness of rail weld, which is equivalent to *d* for a theoretical rail weld, is 0.2 mm according to China's existing maintenance regulation for 300 km/ h high-speed railway. Under this depth, the relationship between the geometric gradient and the wavelength is presented in Fig. 3. As can be seen, the gradient is decreased sharply at first with the increasing wavelength; and then the change is gentle.

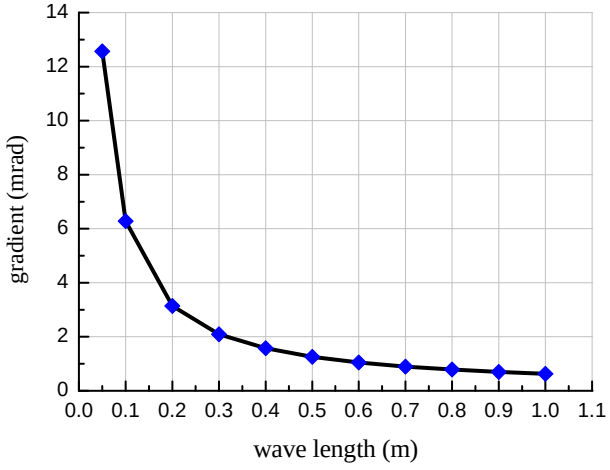

Fig. 3 The relationship between the wave length and gradient under the depth of 0.2 mm

2.3 QI method: assessment of rail weld based on the geometric gradient

(Steenbergen 2006) deduced and validated a mathematical expression of rail welding's geometric gradient and its stimulated maximum wheel-rail dynamic force $F_{dyn,\max}$ in a linear relation,

$$\begin{cases} F_{dyn,\max} = k \cdot \left| dz / dx \right|_{\max} \\ F_{dyn,\max} = F_{\max} - F_{static} \end{cases} \tag{3}$$

Where, $F_{\max}$ and F_{static} are the maximum wheel-rail force and the static wheel load, respectively; *k* is a dimensionless parameter and varies for different running speed of vehicle.

The gradient corresponding to $F_{dyn,\max}$ of 11 kN is regarded as the intervention value *I* to control the irregularity,

$$I = \frac{11}{k} \tag{4}$$

QI (Quality Index) value is defined as the ratio of the maximum geometric gradient and the intervention value. It's obvious that the rail weld with a QI value less than 1 meets the criteria.

2.4 3D high-speed wheel-rail rolling contact FE model

As vehicle speed increases, wheel-rail high-frequency vibration, which vibrates as local deformation, inspired by short wavelength irregularity cannot be ignored. To represent this characteristic, wheel and rail should be modelled as solid element, but not beam as in traditional vehicle-track coupling dynamics model. On the other hand, the stiffness coefficient of the normal contact spring used in the traditional vehicle-track coupling dynamics model is generally derived from the Hertz theory based on the static hypothesis, which contains some differences when dynamic interaction between wheel and rail is taken into account. Based on the above two considerations, a 3D high-speed wheel-rail rolling contact FE model (hereinafter referred to as rolling model) is established in the section to accurately solve the dynamic contact behavior at the rail welds.

The established rolling model based on Chinese high-speed railway is shown in Fig. 4. Considering the vehicle-track system is symmetrical along the center line of the track, only half of wheelset and track were simulated to improve the computational efficiency. Due to the vibration isolation of secondary suspension, the sprung mass was simplified as a mass and connected to the wheel by the primary suspension. The simulated ballastless track contained rails, fastening and slab.

In order to reflect the high-frequency vibration response of the wheel-rail system, the solid element was used for meshing the wheel and rail; also, the non-uniform meshing was imposed to lower the model scale. The minimum element size was 1.1 mm in wheel-rail contact surface. The profiles of wheel and rail were respectively modelled as LMa and CN60, and the track cant of 1:40 was considered. The rolling contact between the wheel and rail were solved in the time domain by the "surface to surface" contact algorithm. The fastening system is simulated by a spring-damping coupling element. In addition, track slab also adopt 8-node solid elements to divide the grid to fully reflect its vibration characteristics. Parameters of each component are obtained from (Zhao 2014).

With smooth wheel-rail surface upon mesh generation, the 3D geometry irregularity at rail weld was applied through modifying coordinate of related nodes on the rail surface by self-compiled program. A series of theoretical and measured

geometries were simulated in the paper. For the theoretical geometry, the vertical coordinate *z* in the longitudinal direction is shown in the Eq. (1), while the measured geometry is taken from measurement on field test (see section 3.2). The horizontal geometry is distributed in parabolic type, whose function is expressed as follows,

$$z = [1-(y/w)^2]\cdot\delta \tag{5}$$

Where, *w* is a half the weld width, which is obtained as 15mm according to the site experience.

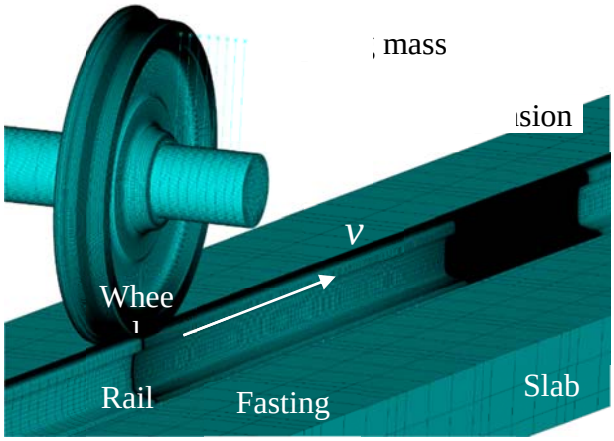

Fig. 4 3D wheel-rail rolling contact finite element model

Implicit-explicit analysis was adopted in the simulation to treat the wheel-rail rolling contact behaviour. Specifically, it firstly adopts implicit algorithm to solve the static contact in the initial position of wheels, and then initialize the explicit rolling contact calculation with the vehicle rolling forwards at a constant speed *v*. Boundary conditions imposed in the model include: constraint of lateral movement on the front of the wheel axle, as well as the longitudinal ends of rail; fixed the bottom of slab, and only vertical movement is allowed for primary suspension and fastening.

3 RELATION BETWEEN GEOMETRIC GRADIENT AND WHEEL-RAIL FORCE, AND ITS APPLICATION FOR MEASURED IRREGULARITIES OF RAIL WELDS

3.1 Explicit finite element analysis of wheel-rail force at theoretical rail welds

The wheel-rail dynamic force (the difference between the wheel-rail force and static load, hereinafter referred to as dynamic force) inspired by the rail weld at a speed of 300 km/ h is shown in Fig. 5. The wave depth of the weld is 0.2 mm with wave lengths of 0.05 m and 0.5 m. Taking the condition of 0.05 m as an example, the impact of dynamic force is caused by the geometric irregularities of rail weld with the maximum value of 91.2 kN, and then fluctuates after passing over the weld. By contract, the dynamic force vibrates gently in the case of 0.5 m, because the long irregularity is difficult to stimulate the high-frequency vibration of the vehicle-track system.

The variation of maximum dynamic force with the gradient is presented in Fig. 6, covering three wave depths of 0.1, 0.2 and 0.3 mm with wave length ranging from 0.03 to 1 m. The condition of 0.2 mm wave depth is illustrated as an example. When the gradient is less than 4.19, the maximum dynamic force and the gradient are presented in linear changes. The linear fitting formula is expressed as shown in the figure (the

slope of the formula is *k* in the Eq. (3)). With the increase of the gradient, the non-linearity of the curve is gradually strengthened to reach the extreme value of 92 kN, which is further increased as the wave depth increases. When the wave depth is 0.3 mm, the extreme value is 133.5 kN and close to the safety limit (150 kN). Hence, the straightness of rail welds should be controlled within 0.2 mm at the speed of 300 km/h to ensure adequate margins for safety. This point of view can be proved by no occurrence of broken rails in the service cycle of Chinese high-speed railway. For easy engineering application, the curve of geometrical gradient- dynamic force has been fitted at different depths. The expression is presented as follows:

$$\left.\begin{aligned} y_{0.1} &= 0.0332g^3 - 1.2611g^2 + 14.2623g - 1.0383 \\ y_{0.2} &= 0.0102g^3 - 0.7002g^2 + 14.7074g - 2.4188 \\ y_{0.3} &= 0.0049g^3 - 0.4848g^2 + 14.7246g - 3.5505 \end{aligned}\right\} \quad (6)$$

Where, $y_{0.1}$, $y_{0.2}$ and $y_{0.3}$ represent the dynamic force of the depth ranging from 0.1 to 0.3 mm; *g* is the geometric gradient.

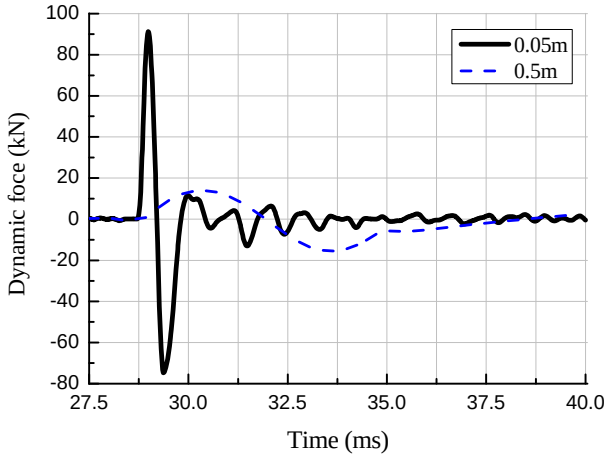

Fig. 5 Variation of dynamic force with time under 300 km/h

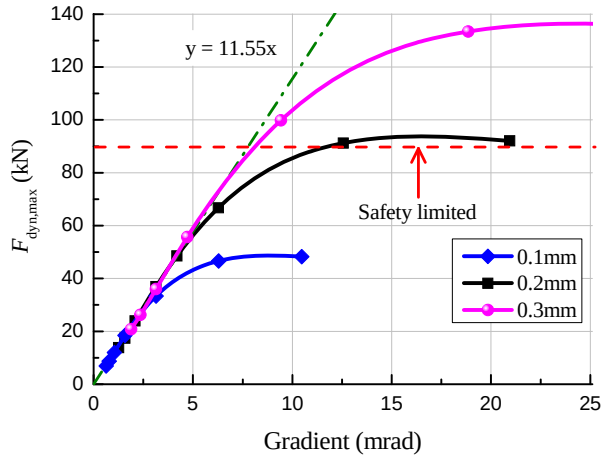

Fig. 6 The change of maximum dynamic force with the gradient under three wave depths

Fig. 7 gives the change of maximum dynamic forces with the gradient under the speed range from 200 to 400 km/ h, and the wave depth of the weld is selected as 0.2mm. With the increase of the speed, the non-linearity of the curve gradually enhances. The corresponding gradient threshold value of the linear region decreases from 6.28 to 3.14, while the slope increases from 7.78 to 15.7. Based on these results, the intervening values defined in formula (4) at 200~400 km/h are 1.41, 0.95 and 0.7, respectively. According to the criteria proposed by RAILPROF, the intervention values are 1.3 and 1 for 200 and 300 km/h, respectively. Obviously, the results obtained from the rolling model are almost the same as the values proposed by RAILPROF that has been used to assess rail welds. So the curve relationship between the dynamic force and the gradient curve obtained by the theoretical geometries is reliable and can be applied to acquire dynamic force at measured rail welds.

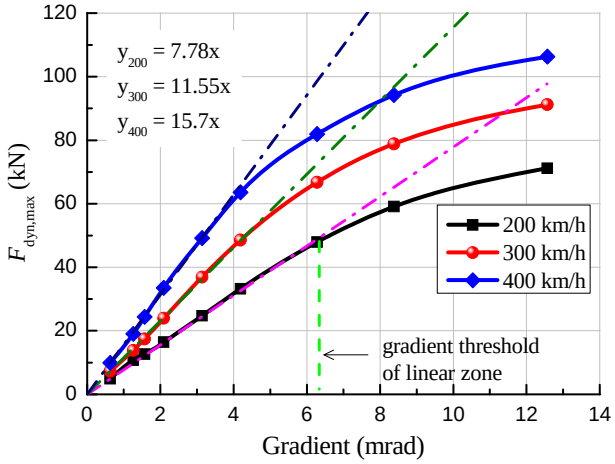

Fig. 7 The influence of the speed on the dynamic force

3.2 Evaluation of dynamic force at measured rail welds and its evolution

The discussion of the above results was based on the theoretical rail welds to facilitate the analysis of the dynamic feature. However, weld irregularities observed on site are often complex. In this section, the focus is to evaluate dynamic force of several rail welds measured in 300 km/h high-speed railway. The evolution of rail welds in the life cycle has been also discussed.

3.2.1 Case 1

As described in Section 2.3, the QI method is used for judging whether the dynamic force at the rail weld is more than 11 kN. This indicator is generally used for the quality assessment of new built lines or after maintenance. Such a low dynamic force can ensure an adequate safety margin. As shown in Fig. 8, it is an early weld geometry (named I) measured in the 300 km/ h high-speed railway and its gradient change is also included with a maximum gradient of 1.33. As the gradient is greater than the intervening value (0.95) shown in Fig. 7, which means no conform to the criteria according to the QI method. Thus, grinding should be carried out to ensure high track comfort.

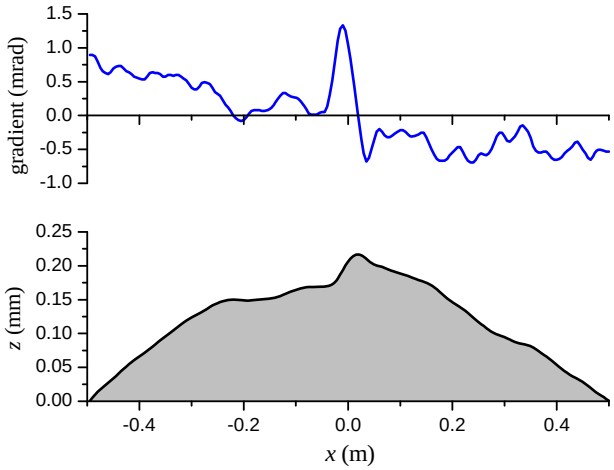

Fig. 8 Measured welds and the gradient distribution

3.2.2 Case 2

Due to the repeated rolling of the wheels, the surfaces of the rail welds will gradually form local irregularities. The dynamic force excited by such a rail weld is generally greater than the limit (11 kN) stipulated in the QI method. For the geometric irregularities appeared in daily operations, its dynamic force shall not exceed 90 kN to ensure the riding safety. The evaluation of the dynamic force for this kind of weld has been elaborated in this section.

The rail weld shown in Fig. 9 is a complex irregularity, named as M. The maximum gradient and excited dynamic forces in 300km/ h are 4.69 mrad and 42.95 kN, respectively. As the change of dynamic force is almost consistent with that of the geometric gradient, results of the dynamic force will not be shown in the following parts to save the layout.

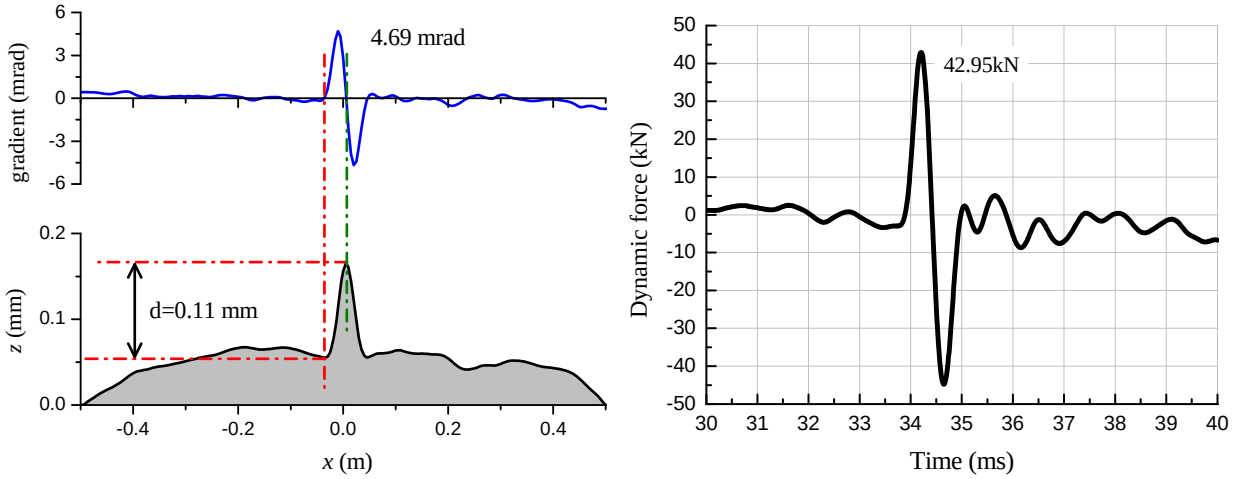

Fig. 9 The gradient (left) and excited dynamic force (right) by measured rail weld M

It is noted that the result of M is located in the curve of the gradient and dynamic force at a depth of 0.1 mm in Fig. 6, although its straightness is 0.1652 mm. This is related to the characteristic depth of the actual geometry of the weld and an approach is proposed below to identify this depth.

As stated in section 2.2 and shown in Fig. 2, there are three zero values for the gradient which are corresponding to the starting point, the peak point and the ending point of the rail weld. Of which, the starting and peak points determine the depth *d* of the geometry. The author marked this characteristic depth for M in Fig. 9, and the value is 0.11 mm. It well explains the reason where the weld's result is located in Fig. 6. Thus, even if the weld straightness can be 0.2 mm, its characteristic depth will be still less than 0.2 mm. Therefore, the maximum dynamic force is difficult to reach the limit value (92 kN) shown in Fig. 6. It further explains that the existing straightness method can well make sure the safety service of wheel-rail systems in the welding zones. Meanwhile, the author suggests that it can appropriately relax the requirements of straightness for such welds.

It is necessary to point out that the gradient in the range of 11 kN has a linear relationship with the dynamic force and is independent of the depth, as shown in Fig. 6. Therefore, the early weld mentioned in section 3.2.1 can be judged directly with the QI method for its small gradient.

3.2.3 Case 3 and 4

Because of high temperature welding, materials in welds and heat affected zone are often different from the base metal, reflecting in low yield strength and hardness. Therefore, materials in that zone are prone to a low collapse due to plastic deformation or wear. Its manifestation is shown in Fig. 10. The gradients of these two welds are 4.34 mrad and 5.72 mrad, respectively. Corresponding dynamic force excited is 45.67 kN and 60.86 kN. These two diagrams also show their characteristic depths as 0.132 mm and 0.208 mm.

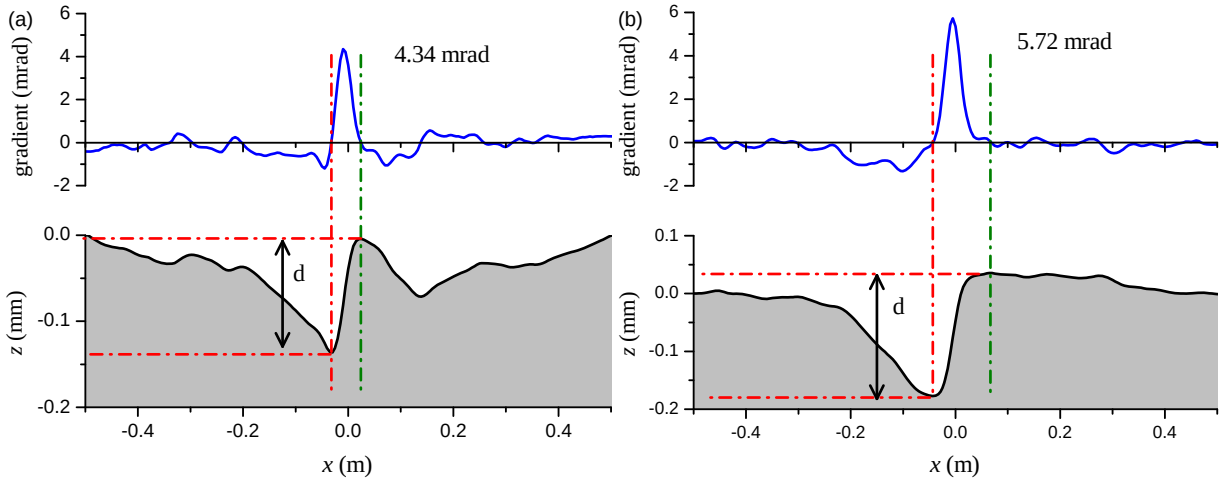

Fig. 10 Two welds (a)L1 and (b)L2 in the later period and corresponding gradient distribution

It should be noted that the characteristic depths of the two welds in Fig. 10 are the same as straightness, which are different from that in Fig. 9. The phenomenon is caused by the opposite direction of the superimposed waveform. In Fig. 9, the principal wave of the weld is convex. Consequently, the complementary wave (or the waveform corresponding to the characteristic depth) of the gradient mutation is also convex. Thus, the characteristic depth is less than its straightness. In Fig. 10, the principal wave of L1

is concave, while the complementary wave is convex. So the principal wave does not affect the depth of the complementary wave. L2 is similar with that.

3.2.4 A postulated rail weld evolution

(Gao 2016) tested 74 sets of rail welds in China's high-speed lines and classified them into three types according to the waveform superimposition, namely the three welds shown in Fig. 9 and 10. It's necessary to note that Fig. 8 and Fig. 9 were classified as the same type in the (Gao 2016). Thus, the four weld geometries of Figure 8 to 10 above are representative. A discussion about evolution of the weld in the life cycle is presented accordingly.

The curve relationship between the gradient and dynamic force at different depths is plotted using Eq. (6), see Fig. 11. Results of the above four welds are also included. Weld I is located in the linear interval of the curve due to its small gradient, which is generally at the beginning stage of life cycle and can only excite small dynamic force. However, due to the maximum slope of the interval curve, that is, the dynamic force will increase significantly with the increase of the gradient. The weld I, if not timely controlled, will gradually evolve into M that the short-wave irregularities will stimulate a high dynamic force. The straightness of the weld will be gradually reduced due to plastic deformation or wear. However, its dynamic effect will maintain stable for a long period. It is because the change of geometric shape in the weld is mainly locates in two softening material zones, i.e. -0.035 m and 0.045 m, as shown in Fig. 9 (a). The complementary wave can be stable for a long time. It can be also seen that the dynamic force grows slowly under the corresponding curve of the depth from the location of M in Fig. 11. Once the weld has evolved into L1 or L2, the rate of deterioration will be increased dramatically. The reason is that the continuous improvement of the straightness of the weld is directly reflected in the increase of the characteristic depth of the complementary wave. On the one hand, the greater the depth, the easier the dynamic force can be improved. That is, even if the L1 gradient is smaller than M, L1 has a higher dynamic force. On the other hand, the deepening depth will significantly increase the gradient, as shown in L2 of Figure 11. Therefore, the weld in the later period should be ground as early as possible, avoiding its continued deterioration leading to rail replacement or even a security accident.

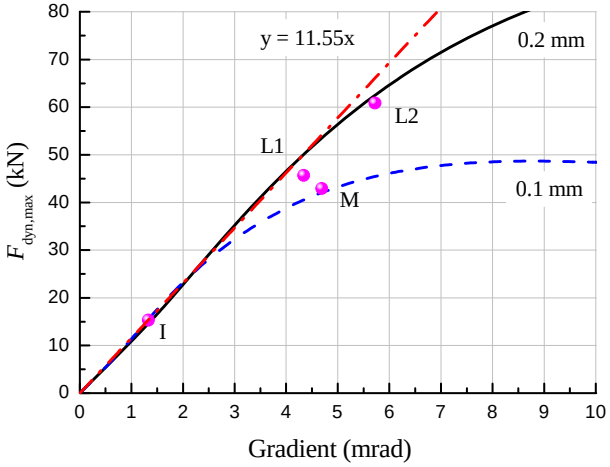

Fig. 11 Distribution of dynamic forces at four rail welds

4 A QUANTITATIVE RELATIONSHIP OF AXLE BOX ACCELERATION AND WHEEL-RAIL FORCE TO ASSESS RAIL WELDS BASED ON MEASURED AXLE BOX ACCELERATION ON SITE

High-frequency vibration generated on the wheel-rail surface under excitation of all kinds of irregularities can be easily transferred to the axle box due to large contact stiffness among wheel tracks. However, previous studies on the axle box acceleration (Zhai 2015) have only focused on the use of response of the axle box acceleration (ABA) in frequency domain to monitor defects without any threshold proposed for safety running. In this section, the rolling model developed in section 2.4 has been utilized to solve the dynamic response of the ABA at rail weld and to establish the quantitative relationship with the dynamic force. Safety limits during the vehicles' running have been proposed from the view of the ABA.

When the vehicle is running at the speed of 300 km/ h, the time course changes of ABA excited by the weld (with the wavelength and the wave depth of 0.1 m and 0.2 mm, respectively) is shown in Fig. 12. Taking into account ABA signals measured on site are often processed through the low-pass filter (LPF) to eliminate the high-frequency noise interference, 1500Hz LPF change is imposed on the simulated result for the application in the processing of measured data. When passing the weld, ABA show a strong vibration and the maximum value is 190.7 m/s^2. Compared with results in Fig. 5, only one impact is occurred in the dynamic force, while the ABA is vibrated continuously. That is to say, acceleration as the second-order derivative of displacement is more sensitive to the rolling-impact shock behavior.

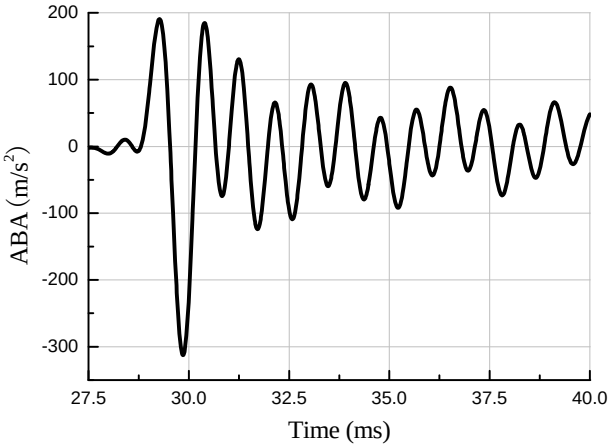

Fig. 12 The response of axle box acceleration under excitation of rail weld

Taking into account of the cases in Eq. 7 (a), the relationship between the ABA and the maximum dynamic force is established, as shown in Fig. 14. Corresponding fitting curve is expressed in Eq. (7),

$$F_{dyn,max} = 0.41 \cdot \mathrm{ABA} \tag{7}$$

The figure shows that the corresponding ABA against the safety limit of 90 kN is 220 m/ s^2. The relationship between ABA and $F_{dyn,max}$ at the speeds of 200 km/ h and 400 km/ h is also obtained in this paper. It is found that the expression is almost the

same as that of Eq. (7), which indicates this relationship is not limited by the speed. Therefore, the measured data can be judged whether meets the criteria according to 220 m/s^2, after passing through the 1500 Hz LPF.

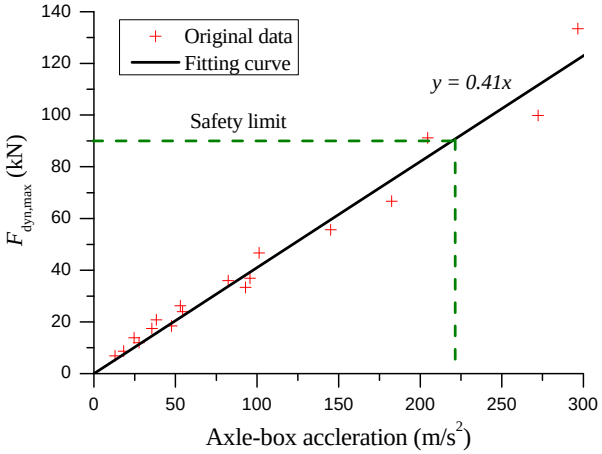

Fig. 13 The relationship between ABA and $F_{dyn,max}$

Fig. 14 gives the curve of the ABA changing along with the running time, which is measured at the speed of 300 km/h in Chinese high-speed railway. 1500 Hz LPF has been imposed on the original signals with consideration of typical frequency range of wheel-rail interaction and noises containing in high-frequency signals. Amplitude of ABA is generally fluctuated within the range of ±50m/s^2 under high-speed rolling conditions on account of existence of irregularities on the surface of wheel and rail. Rails of existing jointless track are welded at an interval of 100 m. Thus, the pulse impulsion will arise every 1.2 s (it's about 100 m by calculating with the speed of 300 km/ h), whose amplitude can reach up to 68 to 163 m/s^2, lowering the safety limit referred in the paper.

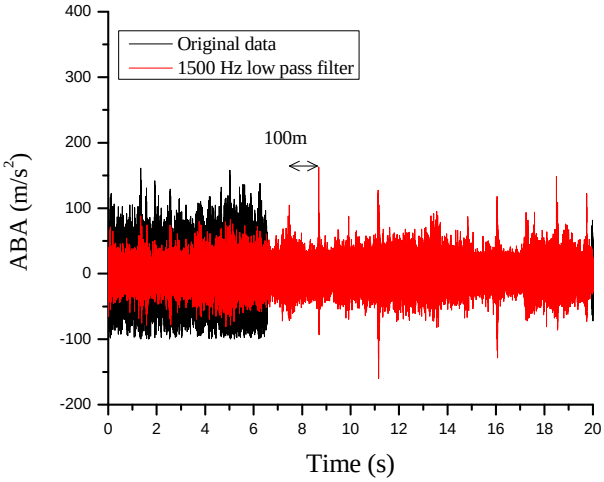

Fig. 14 The response of measured axle box acceleration when a vehicle is operated at the speed of 300 km/h and its 1500 Hz LPF results

5 CONCLUSION

The wheel-rail interaction at theoretical and measured rail welds have been simulated with help of rolling model established in this paper. Considering the maximum depth of 0.2 mm stipulated by the existing straightness regulation, the rolling model established was utilized to solve the dynamic effect of the wavelength welds from 0.03 to 1 m. It is found that the maximum dynamic force is 92 kN or 2.2 times of DAF. It is in line with the actual operating state and proves the rationality of the existing maintenance rules for high-speed railway lines.

When the gradient is small, the dynamic force will be linearly related to the gradient. The improvement of vehicle speed could increase the slope of the linearity. On this basis, the intervention values at the speeds of 200 km/h and 300 km/h are 1.41 and 0.95, which are close to the standard proposed by RAILPROF. Thus, it proved the effectiveness of the numerical values and further proposed the intervention value at the line of 400 km/ h of 0.7.

Based on the measured geometries, the wheel-rail interactions of four typical weld irregularities have been simulated. The evolution process in the life cycle has been discussed on the basis of the geometric characteristics and dynamic effect: Local irregularities were quickly transformed from the geometrical profile of the early weld. The characteristic depth of the irregularity could be developed stably and evolved into a concave form. Soon afterwards, it's quickly developed to the late period.

The quantitative relationship between the dynamic force and ABA (upon 1500 Hz LPF) has been established by the rolling model. It suggests 220 m/ s^2 as the safety limit.

REFERENCES

Gao, J., Zhai, W., & Guo, Y. (2016). “Wheel–rail dynamic interaction due to rail weld irregularity in high-speed railways”. *Proceedings of the Institution of Mechanical Engineers, Part F: Journal of Rail and Rapid Transit*, 0954409716664933.

Grassie, S. L. (1996). “Measurement of railhead longitudinal profiles: a comparison of different techniques”. *Wear*, 191(1-2), 245-251.

Li, Z., Molodova, M., Núñez, A., & Dollevoet, R. (2015). “Improvements in axle box acceleration measurements for the detection of light squats in railway infrastructure”. *IEEE Transactions on Industrial Electronics*, 62(7), 4385-4397.

Liang, B., Iwnicki, S. D., Zhao, Y., & Crosbee, D. (2013). “Railway wheel-flat and rail surface defect modelling and analysis by time–frequency techniques”. *Vehicle System Dynamics*, 51(9), 1403-1421.

Molodova, M., Li, Z., & Dollevoet, R. (2011). “Axle box acceleration: Measurement and simulation for detection of short track defects”. *Wear*, 271(1), 349-356.

Molodova, M., Oregui, M., Núñez, A., Li, Z., & Dollevoet, R. (2016). “Health condition monitoring of insulated joints based on axle box acceleration measurements”. *Engineering Structures*, 123, 225-235.

Steenbergen, M. J. M. M., & Esveld, C. (2006). “Relation between the geometry of rail welds and the dynamic wheel-rail response: numerical simulations for measured

welds". *Proceedings of the Institution of Mechanical Engineers, Part F: Journal of Rail and Rapid Transit*, 220(4), 409-423.

Xiao, G., Xiao, X., Guo, J., Wen, Z., & Jin, X. (2010). "Track dynamic behavior at rail welds at high speed". Acta Mechanica Sinica, 26(3), 449-465.

Zhai W, Liu P, Lin J, et al. (2015), "Experimental investigation on vibration behaviour of a CRH train at speed of 350 km/h". *International Journal of Rail Transportation*, 3(1): 1-16.

Zhao, X., Wen, Z. F., Wang, H. Y., Jin, X. S., & Zhu, M. H. (2014). "Modeling of high-speed wheel-rail rolling contact on a corrugated rail and corrugation development". *Journal of Zhejiang University SCIENCE A*, 15(12), 946-963.